MINISTRY OF EDUCATION AND TRAINING

VIETNAM ACADEMY OF SCIENCE AND TECHNOLOGY

GRADUATE UNIVERSITY OF SCIENCE AND TECHNOLOGY

Nguyen Van Ha

SYNTHESIS OF NOVEL HETEROCYCLIC COMPOUNDS BASED ON THE KNOEVENAGEL CONDENSATION OF 1,3-DIKETONE SYSTEMS AND EVALUATION OF THEIR BIOLOGICAL ACTIVITY

SUMMARY OF DISSERTATION ON SCIENCES OF MATTER

Major: Organic Chemistry

Code: 9 44 01 14

Ha Noi - 2026

The dissertation is completed at: Graduate University of Science and Technology, Vietnam Academy Science and Technology

Supervisors:

1. Supervisor 1: Prof. Dr. Nguyen Van Tuyen - Graduate University of Science and technology, Vietnam Academy of Science and Technology

2. Supervisor 2: Dr. Le Nhat Thuy Giang - Institute of Chemistry, Vietnam Academy of Science and Technology

Referee 1:

Referee 2:

Referee 3:

INTRODUCTION

1. The urgency of the dissertation

Cancer and neurodegenerative disorders, particularly Alzheimer's disease, remain major challenges for modern medicine due to their increasing incidence and mortality rates, while current therapeutic agents still suffer from significant limitations in terms of efficacy, toxicity, and drug resistance. Therefore, the research, design, and development of new compounds with potential biological activity is of urgent importance, especially toward the generation of novel lead compounds with unprecedented structural features, multitarget mechanisms of action, and improved biological efficacy.

In medicinal chemistry, heterocyclic compounds bearing quinone and pyrimidine scaffolds have been widely recognized for their broad spectrum of biological activities, including cytotoxic effects against cancer cells and inhibitory activity toward enzymes associated with neurological disorders. However, systematic studies focusing on the synthesis of new derivatives based on these structural frameworks, in conjunction with biological evaluation and computational modeling to elucidate structure–activity relationships, remain limited. In addition, conventional synthetic approaches often involve multistep procedures with moderate yields and do not fully align with the principles of green chemistry.

Based on these practical considerations, this study was undertaken under the title "*Synthesis of Novel Heterocyclic Compounds Based on the Knoevenagel Condensation of 1,3-diketone Systems and Evaluation of Their Biological Activity*", with the aim of discovering new heterocyclic compounds possessing significant biological activity.

2. Research objectives of the dissertation

- Structural design of novel heterocyclic compounds based on the Knoevenagel condensation of 1,3-diketone systems, employing a strategy of incorporating substituents with strong biological interaction potential, in

alignment with the development of lead compounds for anticancer activity and enzyme inhibition.

- Evaluation of cytotoxic activity against several cancer cell lines, acetylcholinesterase (AChE) inhibitory activity, and molecular docking simulations of the synthesized compounds.

3. Research content of the dissertation

- Synthesis of 1-azaanthraquinone derivatives bearing a γ-butyrolactone ring.
- Synthesis of fluorinated chromeno[2,3-d]pyrimidin-4-one derivatives.
- Synthesis of pyrano[2,3-d]pyrimidine derivatives.
- Synthesis of fluorinated pyranonaphthoquinone derivatives.
- Evaluation of cytotoxic activity against cancer cell lines and acetylcholinesterase (AChE) inhibitory activity of the synthesized compounds.
- Molecular docking studies to elucidate the potential mechanisms of action of the synthesized derivatives toward the investigated biological targets.

CHAPTER 1. OVERVIEW

Chapter 1, comprising 18 pages, presents an overview of the literature on aza-anthraquinone, pyranonaphthoquinone, pyrimidine, and fluorine-containing compounds, together with their biological activities; as well as organic synthetic methods oriented toward green chemistry.

CHAPTER 2. RESEARCH METHODS AND EXPERIENCE

Chapter 2, comprising 31 pages, describes in detail the research methods, synthetic procedures, purification processes, reaction yields, and physicochemical properties of the synthesized compounds, including appearance, color, and melting points, as well as detailed spectroscopic data (IR, ^{1}H NMR, ^{13}C NMR, HRMS) and the methods used for evaluating the biological activities of the obtained derivatives.

CHAPTER 3. RESULTS AND DISCUSSION

3.1. Target of the dissertation

This study aims to design and synthesize novel 1-azaanthraquinone, pyranonaphthoquinone, and pyrimidine derivatives via Knoevenagel condensation and domino multicomponent reactions of 1,3-diketone systems (2-hydroxy-1,4-naphthoquinone, 2-amino-1,4-naphthoquinone, cyclohexan-1,3-dione) with other carbonyl compounds (aromatic aldehydes, tetronic acid, enaminones) under microwave irradiation conditions. The synthesized compounds were subsequently evaluated for their biological activities.

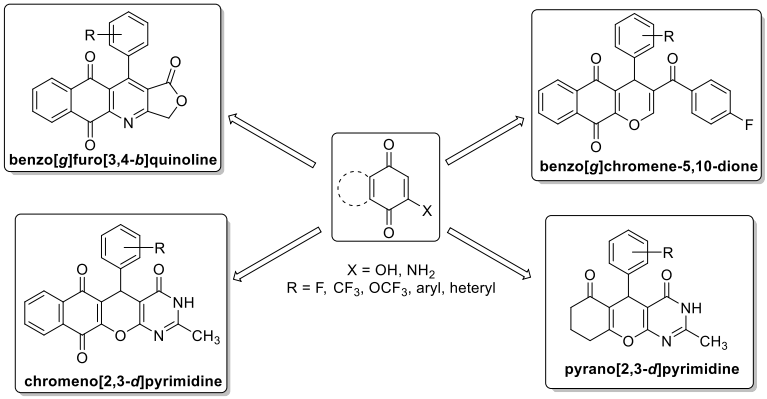

Scheme 3.1. Objectives and synthetic strategy of the study

3.2. Synthesis of 1-azaanthraquinone derivatives bearing a γ-butyrolactone ring

Given the remarkable properties of azaanthraquinone scaffolds and the γ-butyrolactone ring, this study focuses on the synthesis of 1-azaanthraquinone derivatives bearing a γ-butyrolactone moiety through a two-step process: a microwave-assisted three-component reaction, followed by an oxidation–aromatization step.

3.2.1. Synthesis of dihydrobenzo[g]furo[3,4-b]quinoline derivatives

Based on previous reports [29, 94], the dihydrobenzo[g]furo[3,4-*b*]quinoline derivatives **51a–m** were synthesized via a three-component

reaction involving 2-amino-1,4-naphthoquinone (**50**), tetronic acid (**47**), and aromatic aldehydes **48**.

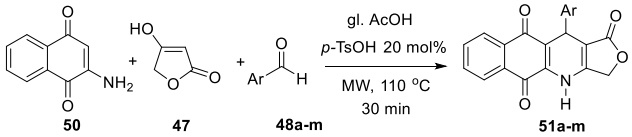

Scheme 3.2. Synthesis of dihydrobenzo[g]furo[3,4-b]quinoline derivatives

The products **51a–m** obtained from these reactions serve as intermediates for the synthesis of 1-azaanthraquinone derivatives bearing a γ-butyrolactone ring

3.2.2. Synthesis of fluorinated 1-azaanthraquinone derivatives bearing a γ-butyrolactone ring

The study investigated the synthesis of 1-azaanthraquinone derivatives bearing a γ-butyrolactone ring (**106a–m**) via oxidation of dihydrobenzo[*g*]furo[3,4-*b*]quinoline derivatives (***51a–m***) using 2,3-dichloro-5,6-dicyano-1,4-benzoquinone (DDQ) as the oxidizing agent.

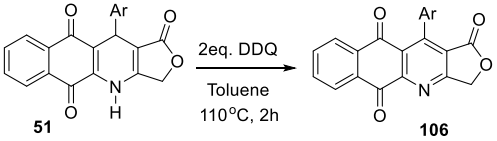

Scheme 3.3. Synthesis of 1-azaanthraquinone derivatives bearing a γ-butyrolactone ring

The reaction was carried out at temperatures ranging from 90 °C to 120 °C over 1–3 hours to evaluate the influence of each parameter on the reaction yield and product purity.

*Table 3.1. Effect of temperature and reaction time on the yield of the aromatization reaction of **51d → 106d** (DDQ/toluene system)*

Entry	Temperature (°C)	Time (h)	Yield (%)	Notes
1	90	2	28	
2	100	2	39	

Entry	Temperature (°C)	Time (h)	Yield (%)	Notes
3	**110**	**2**	**47**	
4	110	1	35	
5	110	3	42	
6	115	2	45	
7	120	2	42	

From the above results, it can be observed that the reaction efficiency is significantly influenced by temperature and reaction time. A temperature of 110 °C and a reaction time of 2 hours were determined to be optimal, allowing the reaction to proceed to completion without causing degradation of the anthraquinone core.

Based on the investigation and optimization of reaction conditions, a total of 13 new compounds (**106a**–**m**) were successfully synthesized with moderate to good yields.

*Table 3.2. Physical properties and yields of compounds **106a–m***

Entry	Comp.	Ar	Color	Melting point (°C)	Yield (%)
1	**106a**	2-Fluoro-4-methoxyphenyl	Brown	210 – 212	43
2	**106b**	3-Fluoro-4-methoxyphenyl	Brown	252 – 254	48
3	**106c**	2,6-Difluoro-4-methoxyphenyl	Brown	190 – 192	46
4	**106d**	2,5-Difluoro-4-methoxyphenyl	Brown	182 – 184	47
5	**106e**	4-Methoxy-2-(trifluoromethyl)phenyl	Brown	244 – 246	45
6	**106f**	2-Fluoro-4-hydroxyphenyl	Brown	310 – 312	48
7	**106g**	4-(Trifluoromethoxy)phenyl	Brown	185 – 187	48
8	**106h**	4-Fluorophenyl	Brown	302 – 304	49
9	**106i**	4-(Trifluoromethyl)phenyl	Brown	204 – 206	45
10	**106j**	2-Fluorophenyl	Brown	251 – 253	43
11	**106k**	2-Methoxy-5-(trifluoromethyl)pyridin-3-yl	Brown -red	-	40
12	**106l**	4-(4-Fluorophenoxy)phenyl	Brown	282 – 284	44
13	**106m**	4-(Difluoromethoxy)-3-hydroxyphenyl	Brown	321 – 323	47

The structures of the obtained compounds were fully elucidated using modern spectroscopic methods, including IR, ^{1}H NMR, ^{13}C NMR, and HR-ESI-MS, with spectral data consistent with the proposed structures.

3.3. Synthesis of chromeno[2,3-d]pyrimidine-4-one derivatives

As discussed in the literature review, fluorine, owing to its high electronegativity, plays an important role in the design of biologically active compounds. The incorporation of at least one fluorine atom or a trifluoromethyl group into bioactive molecules can enhance metabolic stability, membrane permeability, bioavailability, and binding affinity toward target proteins, thereby leading to improved pharmacological activities. Given the notable properties of chromene scaffolds as well as fluorine-containing compounds, this study focuses on the synthesis of chromeno[2,3-*d*]pyrimidine derivatives bearing fluorine atoms.

Initially, the optimal conditions for a four-component domino reaction involving 2-hydroxy-1,4-naphthoquinone (**45**), 4-fluorobenzaldehyde (**116a**), malononitrile (**72a**), and acetic anhydride (**117**) were investigated via a two-step one-pot procedure to synthesize 5-(4-fluorophenyl)-2-methyl-3,5-dihydro-*4H*-benzo[6,7]chromeno[*2,3-d*]pyrimidine-4,6,11-trione (**125a**) (*Scheme 3.4*)

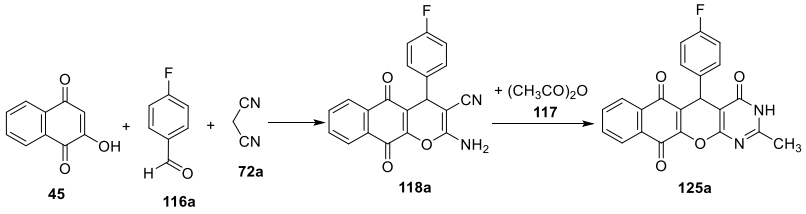

*Scheme 3.4. Synthesis of the compound 5-(4-fluorophenyl)-2-methyl-3,5-dihydro-4H-benzo[6,7]chromeno[2,3-d]pyrimidine-4,6,11-trione (**125a**)*

The study evaluated the effectiveness of several catalysts, and the results are presented in Table 3.3.

Table 3.3. Optimization of catalyst and solvent for the synthesis of compound 125a

Entry	Catalyst	Catalyst loading (mol%)	Solvent	Temperature (ºC)	TLC yield (%)
1	DABCO	5	CH_3CN	82	Vết

Entry	Catalyst	Catalyst loading (mol%)	Solvent	Temperature (°C)	TLC yield (%)
2	DABCO	10	CH_3CN	82	42
3	**DABCO**	**20**	**CH_3CN**	**82**	**80**
4	DABCO	30	CH_3CN	82	75
5	NH_4OAc	20	CH_3CN	82	45
6	Pyridine	20	CH_3CN	82	Vết
7	DMAP	20	CH_3CN	82	62
8	DBU	20	CH_3CN	82	Vết
9	Et_3N	20	CH_3CN	82	Vết
10	DABCO	20	EtOH	78	75
11	DABCO	20	*t*-BuOH	82	71
12	DABCO	20	*i*-PrOH	83	72
13	DABCO	20	Toluene	110	65
14	DABCO	20	EDC	83	62
15	DABCO	20	Chloroform	61	50

The results indicate that the three-component reaction between 1,4-naphthoquinone (**45**), 4-fluorobenzaldehyde (**116a**), and malononitrile (**72a**) afforded the highest yield (80%) when carried out in acetonitrile under reflux conditions with microwave irradiation in the presence of DABCO (20 mol%).

Applying the optimized procedure, a total of 12 chromeno[*2,3-d*]pyrimidine derivatives (**125**) were successfully synthesized, as shown in Scheme 3.5.

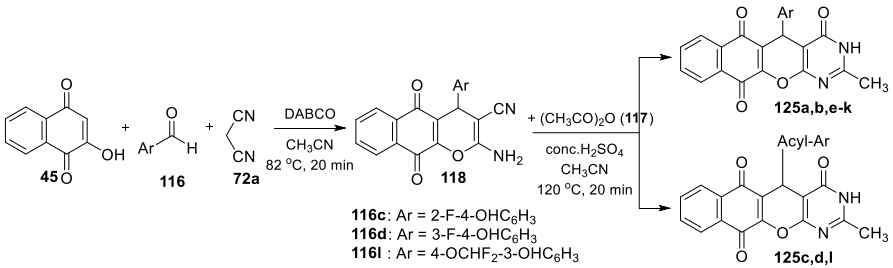

*Scheme 3.5. Synthesis of chromeno[2,3-d]pyrimidine derivatives **125***

*Table 3.4. Physical properties and yields of compounds **125a–l***

Entry	Compound	Ar	color	Melting point (°C)	yield (%)
1	**125a**	4-Fluorophenyl	Yellow	294–296	70
2	**125b**	2-Fluorophenyl	Nâu	233–238	68
3	**125c**	3-Fluoro-4-acetoxyphenyl	Yellow	244–246	60
4	**125d**	2-Fluoro-4-acetoxyphenyl	Yellow	304–306	65
5	**125e**	2,5-Difluoro-4-methoxyphenyl	Yellow	231–233	77
6	**125f**	2,6-Difluoro-4-methoxyphenyl	Yellow	299–301	74
7	**125g**	3-Fluoro-4-methoxyphenyl	Yellow	299–301	80
8	**125h**	2-Fluoro-4-methoxyphenyl	brown-black	225–230	76
9	**125i**	4-Methoxy-2-(trifluoromethyl)phenyl	Yellow - brown	269–271	72
10	**125j**	4-(Trifluoromethoxy)phenyl	brown - red	229–231	79
11	**125k**	4-(4-Fluorophenoxy)phenyl	Yellow	309–311	77
12	**125l**	3-Acetoxy-4-(difluoromethoxy)phenyl	Yellow	279–281	67

3.4. Synthesis of pyrano[2,3-d]pyrimidine-4-one compounds

Within the scope of this study, the synthesis of novel pyrano[2,3-*d*]pyrimidine-4-one heterocyclic compounds was carried out via a two-step domino multicomponent reaction in a single reaction system. The synthetic process consists of two main stages:

(i) Stage 1 – Synthesis of the intermediate 2-amino-4H-pyran-3-carbonitrile
(ii) Stage 2 – Conversion of the intermediate into pyrano[2,3-d]pyrimidine-4-one derivatives

3.4.1. Synthesis of the intermediate 2-amino-4H-pyran-3-carbonitrile

The compound 2-amino-4-methoxy-5-oxo-5,6,7,8-tetrahydro-4H-chromene-3-carbonitrile (**128a**) was synthesized via a three-component reaction from cyclohexan-1,3-dione (**126**), 4-methoxybenzaldehyde (**127a**), and malononitrile (**72a**). The reaction was carried out in acetonitrile (CH_3CN) for 20 minutes under reflux conditions with microwave irradiation at 150 W, using equimolar amounts of **127a**, **72a**, and **126**.

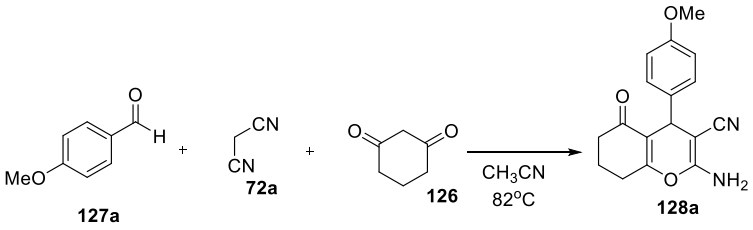

*Scheme 3.6. Synthesis of compound **128a***

3.4.2. Synthesis of pyrano[2,3-d]pyrimidine heterocyclic compounds

Subsequently, the pyrano[2,3-*d]*pyrimidine compound (**142a**) was synthesized via a two-step domino reaction in a one-pot system under microwave irradiation, as shown in *Scheme 3.7*. In the first step, DABCO (2 mol%) was employed as a base catalyst for the three-component reaction between cyclohexan-1,3-dione (1.0 equiv), malononitrile (1.0 equiv), and an aldehyde (1.0 equiv) in acetonitrile. The reaction mixture was stirred at 82 °C for 15 minutes under microwave irradiation, affording the intermediate

2-amino-4H-pyran-3-carbonitrile (**128a**) via a Knoevenagel condensation–Michael addition–intramolecular cyclization sequence.

In the second stage, the intermediate **128a** underwent cyclocondensation with acetic anhydride (117, 3.0 equiv) in acetonitrile, using concentrated H_2SO_4 (0.4 equiv) as a Brønsted acid catalyst to activate the acylating agent. The reaction was conducted at 120 °C for 15 minutes under microwave irradiation, yielding pyrano[2,3-*d*]pyrimidine (**142a**). After completion and purification, compound **142a** was obtained in 78% yield.

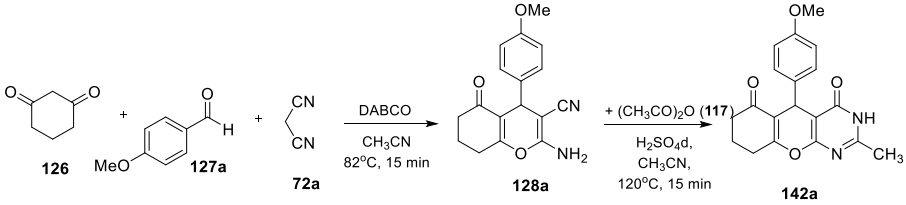

*Scheme 3.7. Synthetic procedure for compound **142a***

Applying the optimized procedure, a total of 11 new pyrano[2,3-*d*]pyrimidine derivatives (**142b–k**) bearing different substituents were successfully synthesized.

3.5. Synthesis of fluorinated pyranonaphthoquinone compounds

To synthesize fluorinated pyranonaphthoquinone compounds, the study investigated the optimal conditions for a three-component reaction involving 2-hydroxy-1,4-naphthoquinone (**45**), 4-(4-fluorophenoxy)benzaldehyde (**143a**), and enaminone (**146**) (Scheme 3.8).

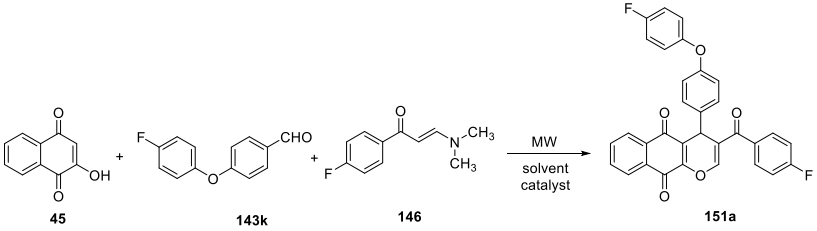

*Scheme 3.8. Synthesis of the derivatives pyranonaphthoquinone **151a***

The study investigated the reaction conditions in various solvents (acetonitrile, ethanol, tert-butanol, propan-2-ol, and toluene) at temperatures ranging from 80 to 120 °C, in the presence or absence of a catalyst. The detailed results are presented in Table 3.5.

*Table 3.5. Effects of solvent, catalyst, and temperature on the synthesis of compound **151a***

Entry	Solvent	Catalyst	Temperature (ºC)	Yield (%)
1	CH_3CN	-	82	-
2	EtOH	-	80	-
3	*t*-BuOH	-	83	-
4	*i*-PrOH	-	83	-
5	Toluene	-	110	-
6	CH_3CN	gl. AcOH (20 mol%)	82	15
7	EtOH	gl. AcOH (20 mol%)	80	24
8	*t*-BuOH	gl. AcOH (20 mol%)	83	29
9	*i*-PrOH	gl. AcOH (20 mol%)	83	25
10	Toluene	gl. AcOH (20 mol%)	110	32
11	gl. AcOH	-	120	76
12	**gl. AcOH**	**-**	**110**	**77**
13	gl. AcOH	-	100	61
14	gl. AcOH	-	90	56

Based on the results obtained for the synthesis of derivative **151a**, a series of pyranonaphthoquinone derivatives (**151a–e**) were successfully synthesized with yields ranging from 71 to 79%, as presented in *Table 3.6*.

*Table 3.6. Physical properties and yields of compounds **151a–e***

Entry	Compound	R	Color	Melting point (ºC)	Yield (%)
1	**151a**	O(4-FC_6H_4)	Yellow	270	77
2	**151b**	2-F	Yellow	279	74
3	**151c**	4-CF_3	Yellow	265	73

Entry	Compound	R	Color	Melting point (°C)	Yield (%)
4	**151d**	4-Cl	Yellow	275	79
5	**151e**	3-NO_2	Yellow	264	71

3.6. Biological activity evaluation of the synthesized compounds

The objective of the biological evaluation was to determine the in vitro cytotoxic potential of the synthesized compounds, while preliminarily analyzing the structure–activity relationships (SAR) to clarify the role of each heterocyclic scaffold and the influence of substituents on the biological activity. The selection of representative cancer cell lines (KB, HepG2, A549, MCF-7) enables the assessment of antiproliferative activity across different cancer types and provides insight into target selectivity.

3.6.1. Cytotoxic activity evaluation of 1-azaanthraquinone derivatives bearing a γ-butyrolactone ring (106a–m)

In the following part of this study, HepG2 (liver cancer), KB (epidermoid carcinoma), A549 (lung cancer), and MCF-7 (breast cancer) cell lines were employed to evaluate the cytotoxic activity of the newly synthesized γ-butyrolactone-fused azaanthraquinone derivatives (compounds **106**).

The cytotoxicity results revealed that most compounds in the 106a–m series exhibited inhibitory effects on cancer cell proliferation at varying levels, as shown in *Table 3.7.* Notably, 10 out of 13 compounds displayed IC_{50} values in the range of 5.77–34.93 μM, indicating a relatively broad spectrum of activity across all four tested cell lines (KB, HepG2, A549, and MCF-7).

*Table 3.7. Cytotoxicity of synthesized compounds **106a–m** against KB, HepG2, MCF-7, and A549 cell lines*

Entry	Comp	Value IC_{50} (μM)			
		KB	HepG2	A549	MCF7
1	**106a**	31.34 ± 1.05	26.53 ± 0.80	22.58 ± 1.08	17.13 ± 1.62

Entry	Comp	Value IC_{50} (μM)			
		KB	HepG2	A549	MCF7
2	**106b**	> 41.10	> 41.10	> 41.10	34.93 ± 1.75
3	**106c**	26.88 ± 1.08	22.93 ± 0.56	17.53 ± 1.37	14.48 ± 0.34
4	**106d**	24.72 ± 0.69	20.97 ± 1.13	**5.77 ± 0.17**	14.95 ± 1.08
5	**106e**	22.42 ± 0.93	22.12 ± 0.91	**6.58 ± 0.25**	17.32 ± 0.59
6	**106f**	32.21 ± 1.04	28.54 ± 1.01	24.91 ± 1.47	18.68 ± 0.56
7	**106g**	25.86 ± 1.11	20.38 ± 1.11	14.27 ± 1.39	12.79 ± 0.19
8	**106h**	23.63 ± 1.48	28.05 ± 0.89	8.96 ± 0.39	19.84 ± 2.03
9	**106i**	21.91 ± 1.42	18.67 ± 1.25	**5.81 ± 0.27**	15.64 ± 1.66
10	**106j**	31.87 ± 0.81	31.37 ± 1.42	9.21 ± 0.31	16.20 ± 1.92
11	**106k**	> 36.34	> 36.34	23.26 ± 1.54	25.23 ± 1.43
12	**106l**	> 35.44	> 35.44	> 35.44	25.10 ± 0.40
13	**106m**	25.18 ± 1.20	21.66 ± 1.09	21.19 ± 1.44	14.39 ± 0.31
14	Ellipticine	1.75 ± 0.08	1.75 ± 0.08	1.79 ± 0.08	1.79 ± 0.08

3.6.2. Cytotoxic activity of fluorinated chromeno[2,3-d]pyrimidine derivatives

The cytotoxic activity of chromeno[2,3-*d*]pyrimidine derivatives (**125a–l**) was evaluated using the MTT assay against human cancer cell lines, including KB (epidermoid carcinoma), A549 (lung cancer), HepG2 (liver cancer), and MCF-7 (breast cancer), as well as the normal cell line HEK-293. Ellipticine, a clinically used anticancer agent, was employed as the reference compound.

As presented in *Table 3.8*, compounds **125b**, **125c**, **125d**, **125g**, and **125l** exhibited strong inhibitory activity against the A549 lung cancer cell line, with IC_{50} values of 7.72 ± 0.63, 2.02 ± 0.17, 8.67 ± 0.77, 8.60 ± 0.81, and 1.76 ± 0.23 μM, respectively. Notably, compound **125l** showed activity comparable to ellipticine (IC_{50} = 1.66 μM). Compounds **125b**, **125c**, and **125g** also demonstrated good inhibitory activity against the MCF-7 breast

cancer cell line, with IC_{50} values of 7.80 ± 0.74, 2.69 ± 0.26, and 9.52 ± 0.84 µM, respectively.

For the KB and HepG2 cancer cell lines, compounds **125b**, **125c**, and **125g** exhibited IC_{50} values in the range of 6.14–9.86 µM. The remaining compounds showed weak inhibitory activity against all four cancer cell lines (IC_{50} > 9 µM). In addition, compounds **125a–l** displayed lower cytotoxicity toward the normal HEK-293 cell line, with IC_{50} values greater than 22.5 µM. Overall, compounds **125c** and **125l** can be considered the most promising candidates among the tested compounds, particularly against A549 and MCF-7 cell lines.

*Table 3.8. Cytotoxic activity results of compounds **125a–l***

Entry	Comp	Value IC_{50}, µM				
		KB	**A549**	**HepG2**	**MCF7**	**Hek-293**
1	**125a**	61.21 ± 4.87	20.60 ± 1.96	61.52 ± 5.59	56.91 ± 5.79	73.88 ± 7.18
2	**125b**	9.86 ± 0.71	7.72 ± 0.63	8.96 ± 1.03	7.80 ± 0.74	32.32 ± 3.22
3	**125c**	8.35 ± 0.76	**2.02 ± 0.17**	6.14 ± 0.52	**2.69 ± 0.26**	28.36 ± 2.60
4	**125d**	42.72 ± 4.85	8.67 ± 0.77	52.20 ± 6.26	53.76 ± 6.58	> 71.69
5	**125e**	55.00 ± 4.74	> 73.33	> 73.33	> 73.33	> 73.33
6	**125f**	> 73.33	57.29 ± 5.27	> 73.33	> 73.33	> 73.33
7	**125g**	9.69 ± 0.71	8.60 ± 0.81	9.81 ± 0.98	9.52 ± 0.84	> 76.49
8	**125h**	> 76.49	> 76.49	> 76.49	> 76.49	> 76.49
9	**125i**	> 68.32	37.45 ± 4.04	> 68.32	> 68.32	> 68.32
10	**125j**	> 70.43	> 70.43	> 70.43	> 70.43	> 70.43
11	**125k**	45.73 ± 4.56	50.33 ± 4.18	41.48 ± 3.31	47.00 ± 4.87	47.16 ± 5.14

Entry	Comp	Value IC_{50}, µM				
		KB	A549	HepG2	MCF7	Hek-293
12	**125l**	23.47 ± 2.58	**1.76 ± 0.23**	23.73 ± 2.02	24.57 ± 2.29	22.50 ± 2.25
13	Ellipticine	1.26 ± 0.12	1.66 ± 0.20	1.75 ± 0.16	1.46 ± 0.12	4.75 ± 0.65

Comparison with ellipticine (reference compound)

Ellipticine (IC_{50} ≈ 1.3–1.8 µM) is a potent reference compound but exhibits relatively high cytotoxicity toward normal cells (HEK-293 ≈ 4.75 µM). In contrast, compounds **125c** and **125l** display comparable anticancer activity while demonstrating significantly improved safety profiles (HEK-293 IC_{50} = 28.36 ± 2.60 µM and 22.50 ± 2.25 µM, respectively). These findings indicate that the structural design strategy incorporating fluorine and acetyloxy substituents on the chromeno[2,3-*d*]pyrimidine scaffold is rational and of practical significance.

3.6.3. Cytotoxic activity of pyrano[2,3-d]pyrimidine derivatives

The results presented in *Table 3.9* indicate that all synthesized pyrano[2,3-*d*]pyrimidine derivatives exhibited no significant cytotoxicity toward the tested cell lines, with IC_{50} values greater than 85 µM across all three cell lines. In contrast, ellipticine showed strong cytotoxicity with IC_{50} values of approximately 1.3–1.8 µM.

These findings suggest that the fused pyrano[2,3-*d*]pyrimidine scaffold in the investigated compounds does not inhibit cancer cell proliferation, indicating a high level of biological safety and a lack of cytotoxic effects at the tested concentrations.

Table 3.9. Cytotoxic activity results of compounds 142a–k

Entry	Comp	Ar	Value IC_{50} (µM)		
			KB	HepG2	A549
1	**142a**	4-$CH_3OC_6H_4$	> 85	> 85	> 85
2	**142b**	4-$CH_3C_6H_4$	> 85	> 85	> 85

Entry	Comp	Ar	Value IC_{50} (μM)		
			KB	HepG2	A549
3	**142c**	4-BrC_6H_4	> 85	> 85	> 85
4	**142d**	4-$CF_3C_6H_4$	> 85	> 85	> 85
5	**142e**	4-ClC_6H_4	> 85	> 85	> 85
6	**142f**	3-BrC_6H_4	> 85	> 85	> 85
7	**142g**	2-$NO_2C_6H_4$	> 85	> 85	> 85
8	**142h**	3-$NO_2C_6H_4$	> 85	> 85	> 85
9	**142i**	3-$CH_3OC_6H_4$	> 85	> 85	> 85
10	**142j**	Benzofuran-3-yl	> 85	> 85	> 85
11	**142k**	Benzo[*b*]thiophen-3-yl	> 85	> 85	> 85
12	Ellipticine		1.26 ± 0.12	1.75 ± 0.16	1.66 ± 0.20

3.6.4. Acetylcholinesterase inhibitory activity of pyrano[2,3-d]pyrimidine derivatives

The acetylcholinesterase (AChE) inhibitory activity of pyrano[2,3-*d*]pyrimidine derivatives was evaluated using a modified Ellman's method. The inhibitory activity was expressed as the half-maximal inhibitory concentration (IC_{50}, μM), with donepezil used as the reference compound. The detailed results are presented in *Table 3.10*.

The results indicate that while compounds **142g** and **142k** showed no AChE inhibitory activity (IC_{50} > 85 μM), the remaining compounds exhibited moderate to good inhibitory activity, with IC_{50} values ranging from 6.51 ± 0.50 to 40.8 ± 3.7 μM. Among them, compound 142i demonstrated the strongest AChE inhibition (IC_{50} = 6.51 ± 0.50 μM), although its activity was lower than that of donepezil (IC_{50} = 0.074 ± 0.008 μM).

A preliminary structure–activity relationship (SAR) analysis of compounds **142a–k** suggests that the AChE inhibitory activity is primarily influenced by the substituents on the phenyl ring attached to the pyran

moiety. In general, compounds bearing halogen substituents (e.g., bromo, trifluoromethyl, and chloro groups) on the phenyl ring exhibited enhanced inhibitory activity.

*Table 3.10. AChE inhibitory activity of compounds **142a–k***

Entry	Compound	Ar	IC_{50} (μM, AChE)
1	**142a**	4-$OCH_3C_6H_4$	40.8 ± 3.7
2	**142b**	4-$CH_3C_6H_4$	21.9 ± 2.0
3	**142c**	4-BrC_6H_4	8.94 ± 0.73
4	**142d**	4-$CF_3C_6H_4$	8.13 ± 0.99
5	**142e**	4-ClC_6H_4	23.4 ± 2.6
6	**142f**	3-BrC_6H_4	8.32 ± 0.88
7	**142g**	2-$NO_2C_6H_4$	>85
8	**142h**	3-$NO_2C_6H_4$	22.7 ± 2.4
9	**142i**	3-$OCH_3C_6H_4$	6.51 ± 0.50
10	**142j**	Benzofuran-3-yl	35.6 ± 2.7
11	**142k**	Benzo[*b*]thiophen-3-yl	>85
12	Donepezil		0.074 ± 0.008

3.7. Molecular docking studies

Within the scope of this study, the **106a–m** series was selected for in-depth molecular docking simulations, as this class exhibited the most pronounced cytotoxic activity, with low IC_{50} values (5–10 μM) across multiple cancer cell lines, particularly A549 (non-small cell lung cancer).

To gain further insight into the molecular mechanism of action of compounds **106a–m**, molecular docking studies were performed to investigate their interactions with tubulin, a key molecular target in cancer chemotherapy. In this study, the crystal structure of tubulin complexed with colchicine was retrieved from the Protein Data Bank (PDB ID: 1SA0). The ligand structures (**106a–m**) were geometry-optimized and subsequently

docked into the active site of tubulin using the Lamarckian Genetic Algorithm implemented in AutoDock 4.2.

The results revealed that most compounds occupy the colchicine-binding pocket; however, notable differences were observed in binding orientation and interaction modes. While colchicine typically penetrates deeply into the hydrophobic pocket of the *β*-subunit, the synthesized derivatives tend to interact more extensively with the α-subunit, particularly near the intradimer GTP-binding region (N-site). These findings suggest that the synthesized compounds may disrupt the *α/β* tubulin interface, thereby interfering with microtubule polymerization, consistent with the mechanism of colchicine-binding agents. Compounds **106d**, **106e**, and **106i** exhibited the most favorable binding energies (ΔG = –15.39 to –16.51 kcal·mol^{-1}), indicating significantly higher binding affinity compared to other compounds in the series. These ligands formed 7–10 π–π stacking interactions with residues such as Phe200, Leu255β, and Tyr224, along with hydrogen bonds involving Asn258β and Lys352β, contributing to the stabilization of the ligand–protein complex. Furthermore, deprotonation of the –NH group on the aza-anthraquinone scaffold enhanced hydrophobicity and π–π stacking interactions, thereby increasing complex stability.

To further evaluate metal-coordination potential, additional docking studies were conducted with procaspase-6, a cysteine protease containing a Zn^{2+} ion in its active site. The results showed that compounds **106a–m** exhibited binding energies (ΔG) ranging from –7.85 to –6.27 kcal·mol^{-1}, indicating moderate complex stability. Compounds **106d**, **106e**, **106i**, and **106j** displayed the highest affinities, corresponding to their ability to coordinate the Zn^{2+} ion via two carbonyl oxygen atoms from the γ-butyrolactone ring and the naphthoquinone core, while also forming hydrogen bonds with His121 and Glu200 in the enzyme active site. This

coordination may inhibit procaspase-6 activity, thereby promoting caspase-3/6 activation and triggering apoptotic pathways.

In summary, the consistency between docking results and in vitro experimental data suggests that the cytotoxic activity of the **106a–m** series primarily arises from dual mechanisms, including tubulin inhibition and Zn^{2+} coordination, leading to disruption of cancer cell structure and activation of apoptosis, ultimately resulting in strong antiproliferative effects.

3.8. Prediction of physicochemical properties and ADMET profiles

To assess the potential of further preclinical development, compounds must not only exhibit strong biological activity but also possess physicochemical and pharmacokinetic properties consistent with those required for drug candidates. On this basis, three representative compounds, **106d**, **106e**, and **106i**, were selected for the prediction of ADMET properties and drug-likeness.

*Table 3.11. Drug-like and ADME-Tox properties of **106d**, **106e** and **106i***

Predicted parameters	106d	106e	106i
Drug likeness			
Lipinski	Accept (0 violation)	Accept (0 violation)	Accept (0 violation)
Leadlikeness	Rejection (1 violation)	Rejection (2 violations)	Rejection (2 violations)
PAINS	1 alert (quinone A)	1 alert (quinone A)	1 alert (quinone A)
Absorption			
Bioavailability	≥ 20%	≥ 20%	≥ 20%
Gastrointestinal absorption	≥ 30%	≥ 30%	≥ 30%
Pgp-substrate	No	No	No
LogK_p (skin permeation)	-6.38 cm s^{-1}	-6.09 cm s^{-1}	-5.89 cm s^{-1}
Distribution			
Plasma protein binding	97. 8%	98.6%	97.7%
Volume distribution	0.27	0.36	0.55
Blood-brain barrier (BBB) penetration	No	No	No

Metabolism			
CYP interaction	CYP1A2 inhibitor (0.87) CYP2C8 inhibitor (0.98) CYP2C9 inhibitor (0.75) CYP2C19 inhibitor (0.67)	CYP1A2 inhibitor (0.82) CYP2C8 inhibitor (0.94) CYP2C9 inhibitor (0.78) CYP2C19 inhibitor (0.62)	CYP2C8 inhibitor (0.99) CYP2C9 inhibitor (0.72)
Excretion			
Clearance (CL)	3.07 mL min^{-1} kg^{-1} (low)	4.21 mL min^{-1} kg^{-1} (low)	3.85 mL min^{-1} kg^{-1} (low)
Half-life ($T_{1/2}$)	1.4h (intermediate)	1.1h (intermediate)	1.2h (intermediate)
Toxicity			
hERG blockers	Inactive (0.33)	Inactive (0.45)	Inactive (0.38)
AMES mutagenicity	No (0.48)	No (0.52)	No (0.57)
Rat oral acute toxicity	Low (0.54)	Low (0.48)	Low 0.59)
Eye irritation	No (0.39)	No (0.29)	No (0.45)
Respiratory toxicity	No (0.30)	No (0.49)	No (0.38)

The drug-likeness of three representative biologically active compounds (**106d**, **106e**, and **106i**) was comprehensively evaluated based on predicted physicochemical parameters and ADMET properties using SwissADME and ADMETlab 3.0. The results indicate that most of the 13 core physicochemical parameters fall within the acceptable range for potential drug candidates, with only minor deviations in lipophilicity and aqueous solubility. Although these compounds exhibit relatively high lipophilicity, their logP values (< 5.0) comply with Lipinski's rule of five for orally administered drugs. However, they do not fully meet the criteria for lead compounds due to their relatively high molecular weight and hydrophobicity. All three compounds also showed PAINS alerts associated with the quinone A scaffold, indicating potential assay interference.

Regarding ADMET properties, the compounds are predicted to have high intestinal absorption, are not substrates of P-glycoprotein, and exhibit moderate intestinal permeability with oral absorption exceeding 30%. Skin

permeability is very low, and none of the compounds are predicted to cross the blood–brain barrier, which may reduce the risk of central nervous system-related side effects. Although high plasma protein binding is predicted, the volume of distribution remains within an acceptable range. In terms of metabolism, compounds **106d** and **106e** show a tendency to inhibit multiple CYP450 isoenzymes, suggesting a potential risk of drug–drug interactions. All compounds exhibit low clearance and moderate half-life values, indicating suitability for oral drug development.

In summary, all three compounds are predicted to be non-mutagenic (Ames test), non-hepatotoxic, and non-irritating to the eyes or respiratory system (*Table 3.11*). Overall, these results suggest that compounds **106d**, **106e**, and **106i** possess promising drug-like properties with acceptable safety profiles, supporting their potential as lead compounds for further optimization in anticancer drug development.

CONCLUSIONS AND RECOMMENDATIONS

Conclusions:

1. The dissertation has successfully developed four synthetic protocols affording a total of 41 novel heterocyclic compounds based on the Knoevenagel condensation of 1,3-diketone systems via domino multicomponent reactions, including:

   - 13 1-azaanthraquinone derivatives bearing a γ-butyrolactone ring (**106a–m**), yields: 40–49%.

   - 12 fluorinated chromeno[2,3-*d*]pyrimidin-4-one derivatives (**125a–l**), yields: 60–80%.

   - 11 pyrano[2,3-*d*]pyrimidine derivatives (**142a–k**), yields: 63–81%.

   - 5 fluorinated pyranonaphthoquinone derivatives (**151a–e**), yields: 71–79%.

   The structures of all synthesized compounds were fully elucidated by IR, ^{1}H NMR, ^{13}C NMR, and HRMS.

2. The biological activities of the synthesized compounds were evaluated:

   - Cytotoxic activity against human cancer cell lines KB, HepG2, A549, MCF-7, and the normal cell line HEK-293: 16 out of 36 tested compounds exhibited cytotoxic effects. Notably, five representative compounds (**106d**, **106e**, **106i**, **125c**, and **125l**) showed IC_{50} values in the range of 1.76–6.58 μM, comparable to the reference compound ellipticine (IC_{50} = 1.8 μM) under the same experimental conditions.

   - For acetylcholinesterase (AChE) inhibitory activity of the **142a–k** series, 10 out of 12 compounds exhibited inhibitory effects, with IC_{50} values ranging from 6.51 to 40.8 μM. Among them, compound **142i** showed the strongest activity (IC_{50} = 6.51 ± 0.50 μM).

3. ADMET prediction and molecular docking studies were performed for the **106a–m** series, providing insights into their mechanisms of action and supporting rational drug design. The results indicate that this class of

compounds may act on dual molecular targets, namely tubulin (cell cycle arrest) and procaspase-6 (apoptosis activation). Among them, compounds **106d**, **106e**, and **106i** are considered the most promising candidates and may serve as multitarget-oriented derivatives for further development.

Based on the obtained results, the dissertation has successfully achieved its research objectives through a systematic approach. These findings not only provide scientific significance but also establish a reliable experimental foundation for further studies on mechanisms of action, pharmacokinetic properties, and structural optimization toward future drug development.

Recommendations:

Based on the synthesized compound series and the obtained results, it is recommended to further select and investigate representative structural scaffolds to systematically explore structure–activity relationships. A close integration of synthetic chemistry, biological evaluation, and molecular modeling should be emphasized to clarify the roles of key structural features, thereby guiding the rational design and optimization of new derivatives for future drug development.

NEW CONTRIBUTIONS OF THE DISSERTATION

1. Four synthetic protocols have been developed, and the formation mechanisms of the target products have been elucidated for the synthesis of novel heterocyclic compounds based on the Knoevenagel condensation of 1,3-diketone systems via domino multicomponent reactions under microwave-assisted conditions.
2. For the first time, 41 new heterocyclic derivatives based on the scaffolds of 1-azaanthraquinone bearing a γ-butyrolactone ring, chromeno[2,3-*d*]pyrimidin-4-one, pyrano[2,3-*d*]pyrimidine, and pyranonaphthoquinone have been synthesized and structurally characterized, contributing to the expansion of valuable heterocyclic libraries in medicinal chemistry.
3. The dissertation provides a systematic evaluation of the biological activities of the synthesized compounds, including cytotoxic activity against human cancer cell lines (KB, HepG2, A549, MCF-7) and the normal cell line HEK-293, as well as acetylcholinesterase (AChE) inhibitory activity. The results revealed that 16 out of 36 compounds exhibited cytotoxic activity, among which compounds **106d**, **106e**, **106i**, **125c**, and **125l** showed IC_{50} values in the range of 1.76–6.58 μM, comparable to the reference compound ellipticine. In addition, within the pyrano[2,3-*d*]pyrimidine series, 10 out of 12 compounds exhibited AChE inhibitory activity with IC_{50} values ranging from 6.51 to 40.8 μM, with compound **142i** showing the most potent activity.
4. Based on molecular docking and ADMET predictions, the dissertation has preliminarily elucidated the interaction potential of 1-azaanthraquinone derivatives bearing a γ-butyrolactone ring with relevant molecular targets, indicating their potential dual action on tubulin and procaspase-6. Compounds **106d**, **106e**, and **106i** have been identified as the most promising candidates, providing a basis for further investigation.

LIST OF PUBLISHED ARTICLES RELATED TO THE THESIS

1. Ha Thanh Nguyen, **Ha Nguyen Van**, Phuong Hoang Thi, Tuyet Anh Dang Thi, Giang Le-Nhat-Thuy, Quynh Giang Nguyen Thi, Anh Nguyen Tuan, Cham Ba Thi, Hung Tran Quang, Tuyen Van Nguyen. Synthesis and Cytotoxic Evaluation of New Fluoro and Trifluoromethyl Substituents Containing Chromeno[2,3-*d]*pyrimidines. *ChemistrySelect*, 2023, 8, e202300227.
   https://doi.org/10.1002/slct.202300227.
2. Ha Thanh Nguyen, Thi Quynh Giang Nguyen, **Ha Nguyen Van**, Thi Phuong Hoang, Nhat Thuy Giang Le, Tuan Anh Nguyen, Thi Cham Ba, Duc Huy Le, Thi Tuyet Anh Dang, Van Kiem Phan, Van Tuyen Nguyen. Synthesis and Evaluation of Acetylcholinesterase Inhibitory and Cytotoxic Activities of Pyrano[2,3-*d*]pyrimidines. *Natural Product Communications*, 2023, Vol. 18(9), 1–10.
   https://doi.org/10.1177/1934578X231201037
3. Ha Thanh Nguyen, **Ha Nguyen Van***, Hai Pham-The, Ket Tran Van, Dao Long Vu, Tuyet Anh Dang Thi, Giang Le-Nhat-Thuy, Quynh Giang Nguyen Thi, Phuong Hoang Thi, Tuan Anh Nguyen, Mai Dang Thi, Julien Braire, Tuyen Nguyen Van. Synthesis, Molecular Docking Analysis, and In Vitro Cytotoxic Evaluation of New Fluorinated γ-Butyrolactone-Aza-Anthraquinone Compounds. *Chemistry & Biodiversity*, 2025; 0:e02030.
   https://doi.org/10.1002/cbdv.202502030
4. Nguyen Ha Thanh, Nguyen Tuan Anh, Le Nhat Thuy Giang, Nguyen Thi Quynh Giang, **Nguyen Van Ha**, Nguyen Thi Nga, Nguyen Thi Hien, Vu Duc Cuong, Dang Thi Tuyet Anh. Microwave-assisted three-component synthesis of new pyranonaphthoquinone derivatives. *Journal of Chemistry and Applications,* 2024, No. 3B (71), pp. 66–71.